

# HIGH GRADIENT TESTING OF THE FIVE-CELL SUPERCONDUCTING RF MODULE WITH A PBG COUPLER CELL\*

S. Arsenyev<sup>†</sup>, Massachusetts Institute of Technology, Cambridge, MA 02139, USA  
 W.B. Haynes, D.Yu. Shchegolkov, E.I. Simakov, T. Tajima,  
 Los Alamos National Laboratory, PO Box 1663, Los Alamos, NM 87545, USA  
 C.H. Boulware, T.L. Grimm, A.R. Rogacki, Niowave, Inc.,  
 1012 North Walnut Street, Lansing, MI 48906, USA

## Abstract

Superconducting radio-frequency (SRF) accelerating structures allow high-gradient operation in continuous-wave mode. These machines can be limited by beam-breakup instability at high currents because higher-order modes with very high Q factors are easily excited by the beam. Photonic band gap (PBG) structures provide a way to strongly damp higher-order modes without compromising the performance of the structure in the fundamental mode.

We first address the design of the structure and issues that arise from incorporating a complex PBG cell into an SRF module. In particular, the module was tuned to have uneven accelerating gradient profile in order to provide equal peak surface magnetic field in every cell. We then cover the fabrication steps and surface treatment of the five-cell niobium structure and report results of the high gradient tests at temperatures of 4 K and 2 K.

## INTRODUCTION

Superconducting radio frequency (SRF) cavities are the natural choice for future generations of high energy linacs, especially for high-duty-factor machines where the heat produced in the accelerating structure cannot be effectively extracted [1]. Going to higher frequencies in SRF cavities is desirable in some applications for various reasons. First, it allows lowering the cost of an accelerator and increasing achievable luminosity of an electron beam. Second, it is necessary for harmonic cavities operating at multiples of accelerator frequency. One example of a high-current linac of relatively high frequency is the proposed SRF harmonic linac for eRHIC [2], which would be used to undo nonlinear distortion of the beam's longitudinal phase space induced by the main linac's waveform.

However, going up in frequency makes higher-order-mode (HOM) wakefields increasingly problematic, as their transverse impact on the beam scales as the frequency cubed [3]. In a high-frequency machine, wakefields destroy quality of the beam and cause beam-breakup instability that leads to beam loss. Thus designs of high frequency SRF accelerators incorporate HOM dampers. We propose to replace one of the conventional elliptical cells with a PBG cell that includes

HOM couplers and a fundamental power coupler (FPC) (see Fig. 1). PBG cells possess intrinsic property of frequency selectivity and can therefore be designed so that only the accelerating mode is selectively confined. The fundamental mode provides acceleration, and HOMs are coupled out.

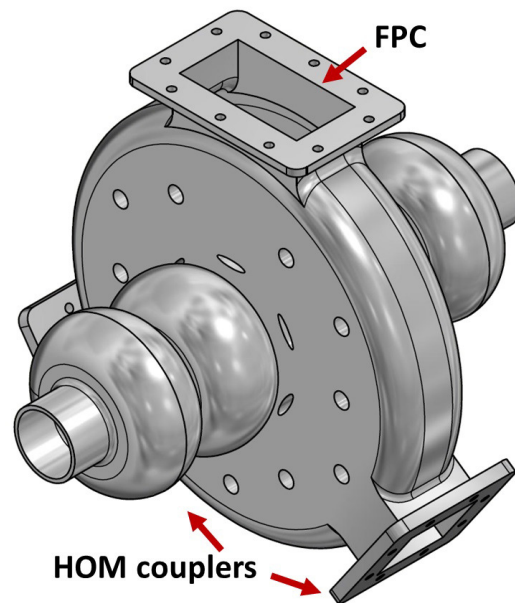


Figure 1: 2.1 GHz 5-cell module with a PBG center cell.

To date, accelerator research has been mostly focused on room temperature PBG cavities. Various designs have been proposed, including metal and dielectric structures [4–6]. In particular, it has been experimentally shown that a room-temperature PBG accelerating module can greatly reduce HOM wakefields [7].

Several tests have previously demonstrated that a high gradient and high Q factor can be achieved in a single superconducting PBG cell [8,9], opening a possibility for building a multi-cell accelerating module. The designed module consists of four elliptical cells and one PBG cell. Using cells of different kinds in one module introduces new challenges such as ensuring that the peak surface magnetic fields in all cells are equal. A niobium 5-cell cavity was made for high gradient testing (see Fig. 3 later).

This paper briefly discusses the design and fabrication of the cavity, and focuses on the high gradient testing. Results of the test are analyzed and discussed. The last section discusses a low Q problem encountered in the first high

\* This work is supported by a DOE Office of Nuclear Physics SBIR grant DE-SC0009523 and the U.S. Department of Energy (DOE) Office of Science Early Career Research Program.

<sup>†</sup> arsenyev@mit.edu

gradient test, and includes a detailed discussion of RF losses in the waveguide joints.

## DESIGN OF THE CAVITY

### Accelerating Properties

The cavity was originally designed for the Los Alamos National Laboratory Navy Free Electron Laser beamline with a beam current of 100 mA and a bunch frequency of 100 MHz. The design also assumed that the cavity was to be powered by a 200 kW 2.1 GHz klystron and provided 2 MV of accelerating voltage.

Similar to the 5-cell module of [10], the elliptical cells were of "low-loss" shape. One elliptical cell was replaced with a PBG cell. HOM couplers and an FPC were attached to the PBG cell. Attaching the waveguides directly to the middle cell is possible because of the low field at the periphery of the PBG cell. This is beneficial to HOM damping and increases real estate gradient by saving space on the beampipes [11].

The PBG cell was detuned to obtain a non-flat accelerating gradient profile [11]. If the gradient profile was flat, performance of the entire accelerator module would be limited by a single PBG cell due to the higher peak magnetic field on the surface of the inner rods.

The inner PBG rods were specifically shaped to minimize  $B_{peak}$ , which allows to achieve gradient as high as 60% of that in elliptical "low-loss" shaped cells (see Fig.4 in the next section). The penalty in accelerating gradient incurred to implement the coupling through the PBG cell is minimal, as shown by the accelerator parameters listed in Table 1.

Table 1: Accelerating Properties of the Module Compared to a Design with 5 Elliptical "Low-Loss" Cells.

	PBG	5 elliptical cells
Frequency $f_0$	2.1 GHz	
Shunt impedance $\frac{R}{Q}$	515 $\Omega$	525 $\Omega$
Geometrical factor $G$	265	276
Peak surface electric field ratio $E_{peak}/E_{acc}$	2.65	2.50
Peak surface magnetic field ratio $B_{peak}/E_{acc}$	4.48 $\frac{mT}{MV/m}$	4.27 $\frac{mT}{MV/m}$

The beamline parameters and the desired accelerating voltage dictate the accelerating mode external (input) Q factor to be  $Q_{ext} = 3.8 \times 10^4$ . Since the accelerating mode is strongly confined in the PBG lattice, one of the rods was removed which resulted in  $Q_{ext} = 2 \times 10^4$ . This rather strong coupling gives us the flexibility to adjust to a particular beam current and RF power values as  $Q_{ext}$  can be increased by means of a waveguide stub.

### Higher Order Modes Damping

We studied HOMs paying particular attention to monopole and dipole modes with frequencies below their re-

spective beam pipe cutoffs (Fig.2). Quadrupoles and modes with even higher order angular variation were not considered because their transverse impact is smaller for the same beam offset. Modes with frequencies above the cutoff are considered less important as they propagate through the beam pipe.

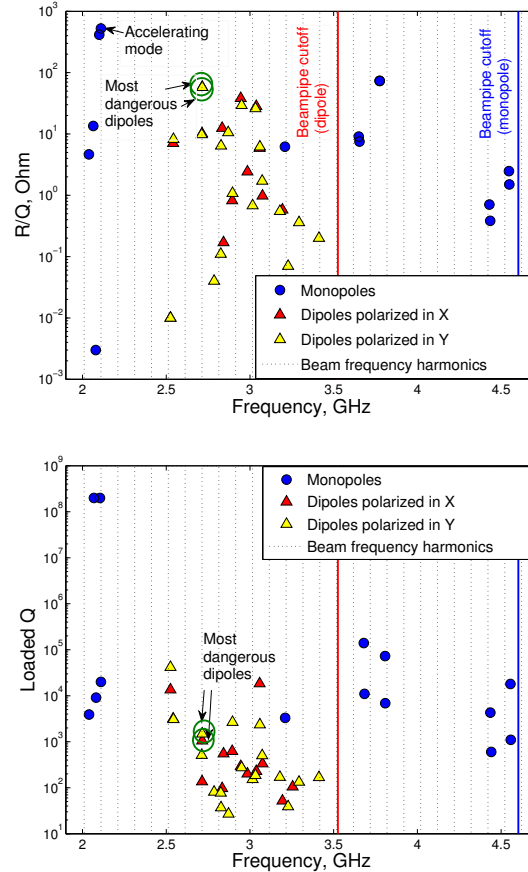


Figure 2: Simulated shunt impedances (top) and loaded Q-factors (bottom) for monopole and dipole modes with frequencies below their respective cutoffs.

We should especially carefully study monopoles that have the potential to be on resonance with a harmonic of the beam frequency. In the adverse case when this happens, resonant build-up occurs after an infinite train of bunches. Due to the fabrication tolerances some frequency uncertainty is inevitable. All the monopoles with frequencies within the uncertainty range of a beam harmonic are considered on resonance. An upper bound was found for the longitudinal voltage kick experienced by a bunch due to all monopoles below the cutoff. For the listed operating parameters, it equals 0.7% of the accelerating voltage.

The dipole modes are of major concern due to their potential to drive transverse beam-breakup instability. Therefore the main goal of the design was to bring down Q-factors of the dipoles with the highest shunt impedances (Fig.2). A detailed analysis of dipole HOMs together with measurements of external Q-factors in a copper prototype of the cavity was

done in [12]. Assuming beam offset equal to 1/4 of the beam pipe radius and calculating  $Q_{ext}$  for each dipole mode, we found an upper bound for the transverse voltage kick due to the dipoles. For the listed operating parameters, it equals 0.3% of the accelerating voltage.

Monopole and dipole modes together constitute less than 5kW of power. The power is extracted by the 3 waveguides and is absorbed by RF loads outside of the cryomodule. Waveguide HOM couplers are well suited for high HOM power as they don't have cooling problems inherent to antenna couplers.

## FABRICATION AND TUNING

The cavity was fabricated by Niowave, Inc (Fig. 3) from a combination of fine-grain niobium sheets and machined ingot parts, joined by electron-beam welding. Two halves of the PBG cell were stamped and then fitted and joined with the PBG array rods. All 5 cells were welded together in a few steps which incorporated tuning to account for the effect of weld shrinkage on field flatness.



Figure 3: The 5-cell cavity for high gradient testing, made from bulk niobium.

Tuning was done by trimming halves of each elliptical cell at the equator. Gradient profile after the final weld was within 5% of the design and no additional tuning was required. Nevertheless, the elliptical cells were squeezed a little in longitudinal direction to even-out the profile. Final gradient profile is shown in Fig 4.

The cavity's Q-factor measured at a room temperature ( $Q_{300K} = 7300$ ) corresponded to niobium bulk conductivity  $\sigma = 6.3 \times 10^6 \Omega^{-1}m^{-1}$  which is in good agreement with theory.

ISBN 978-3-95450-178-6

950

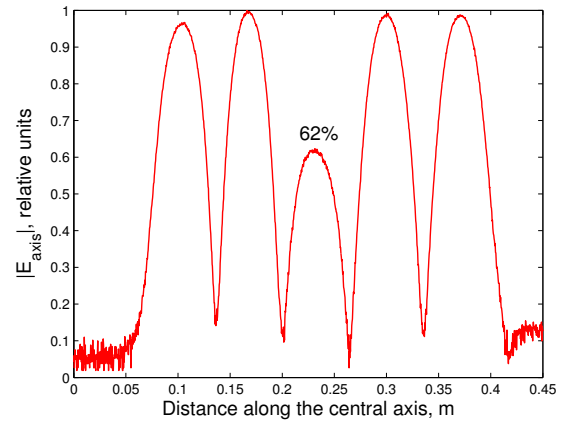


Figure 4: Gradient profile of the tuned cavity obtained from bead-pulling measurements. The field in the center cell is intentionally lowered to ensure equal peak surface magnetic field in every cell.

For a high-gradient test it was not necessary to tune the cavity to exactly 2.100 GHz, therefore the center (PBG) cell was not tuned. Nevertheless, the resulting frequency of the cavity in operation was within 0.5% of the design frequency (2.1062 GHz in liquid helium). In a multi-cavity linac where all the structures must be tuned to the same frequency, a few different mechanisms of tuning have been proposed, including pushing on the inside of the PBG rods. A cavity tuner which stresses and compresses the full cavity to tune the frequency of the structure will affect the field flatness because the elliptical cells will tune much more easily than the center PBG cell. Likely such a scheme would allow sufficient tuning to synchronize a multi-cavity linac with very little cost in terms of field flatness. Prototype tuning and simulations of this effect are planned.

After welding, the cavity was chemically treated using 1:1:2 buffered chemical polish (BCP) solution of HF, HNO<sub>3</sub>, and H<sub>3</sub>PO<sub>4</sub> to etch 150  $\mu m$  of the inner niobium surface, and high-pressure rinsed with ultrapure water, both at Niowave.

The FPC and the two HOM waveguide couplers were covered with niobium plates to provide an RF seal. The plates were clamped between the cavity flanges and stainless steel covers. Aluminum hexagonal gaskets (based on DESY diamond seals) were placed between the waveguide flanges and the stainless steel covers to provide a vacuum seal (Fig. 5).

## HIGH GRADIENT TESTS

The cavity was shipped to Los Alamos, where it was assembled with a pickup probe and an adjustable drive probe (Fig. 5) in a class 100 clean room. Both probes were hollow aluminum rods designed to match the 50  $\Omega$  impedance of coaxial lines. The pickup probe was designed to provide external quality factor  $Q_e = 6 \times 10^{11}$ , and the drive probe was designed to provide  $Q_e$  in the range  $2 \times 10^7 < Q_e < 10^{10}$ . Adjustability was provided by a bellow that could be squeezed or extended to change  $Q_e$  (Fig. 5). A macor

SRF Technology - Cavity

E11-Specialty Cavities

support plate was used to prevent the long drive probe from tilting relative to the axis.

A 200W TWT amplifier provided RF power through the drive probe. A phase lock loop was used to lock the generator's RF frequency to the cavity's resonant frequency.

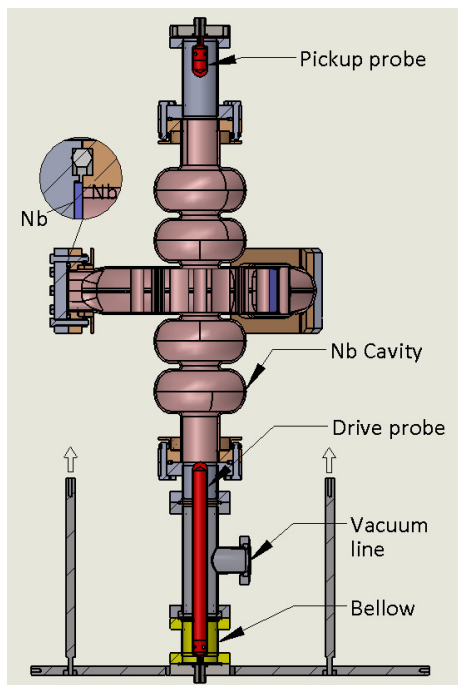


Figure 5: Cross section of the 5-cell module with the pickup assembly and the drive assembly.

The cavity was baked at 120 °C for 2 days. It was then pumped down to  $5 \times 10^{-8}$  Torr before putting it in liquid helium. The cavity was quickly covered with helium to prevent hydrides from forming on the surface (Q-disease). A magnetic field compensating coil was used to compensate for the Earth's magnetic field.

A network analyzer was used to find all but one spatial variations of the monopole mode:  $\pi$ ,  $4\pi/5$ ,  $3\pi/5$ ,  $2\pi/5$  modes. Frequencies of the modes were confirmed with HFSS simulations. The  $\pi/5$  mode is less easily excited by the probe because it has small fields in the end cells.

It was found that even when the drive probe was fully inserted into the cavity (strongest coupling), all 4 modes were highly undercoupled. The coupling to the cavity did not change even after going from a helium bath temperature of 4 K (atmospheric pressure) to 2 K. This indicated that this mode had a very low unloaded Q-factor dominated by non-superconducting losses.

The cavity was pulled out of the cryostat. Longer drive and pickup probes were made for coupling to the low-Q modes (simulated minimum  $Q_{ext}$  of the drive probe was  $1.1 \times 10^5$ ). The RF surface was inspected but no evident defects were found. The cavity was reassembled with the new probes, high pressure rinsed and baked again. The assembly was lowered into the cryostat. The experiment was then repeated at a helium bath temperature of 4 K.

With the new probes, the accelerating mode was still undercoupled. However, this time we could use the phase lock loop to estimate  $Q_0$  for the  $\pi$ -mode from cavity energy decaying time using pulsed excitation:  $Q_{0\pi} = 1.6 \times 10^6$ . It was not possible to feed significant power into the cavity to reach high accelerating fields, so only the anomalous low-field Q value is shown in Fig. 6. Using the same technique,  $Q_0$  for the  $3\pi/5$  mode was found to be even lower:  $Q_{03\pi/5} = 9.3 \times 10^5$ .

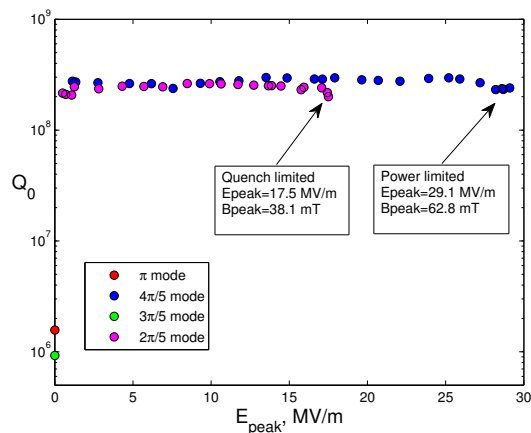


Figure 6: Cavity quality factor for different modes as a function of the peak surface electric field at 4K. The drive probe was adjusted to provide near critical coupling to the modes  $2\pi/5$  and  $4\pi/5$ , or max achievable coupling for modes  $\pi$  and  $3\pi/5$ .

The  $2\pi/5$  and  $4\pi/5$  modes showed much higher Q factors:  $Q_{02\pi/5} = 2.2 \times 10^8$ ,  $Q_{04\pi/5} = 2.7 \times 10^8$ . For each of these two modes, we were able to adjust the drive probe to have near critical coupling ( $\beta \approx 1$ ). We were able to feed up to 135W of power into the cavity and measure  $Q_0$  vs  $E_{peak}$  (plotted in Fig. 6), where  $E_{peak}$  is the peak surface electric field used to compare the relative field levels of modes with very different shunt impedance values.

The maximum achievable field in the  $2\pi/5$  mode was limited by a quench-like behavior with the rapid change in reflected power from near zero to 100% and back. The quench did not cure after a few minutes of conditioning. For the  $4\pi/5$  mode, several similar quenches were processed and we eventually reached the limit of maximum available input RF power. At surface field of about 29 MV/m, rapid increase in X-rays was observed indicating field emission, but was quickly processed. No consistent multipacting barriers were encountered.

### ANALYZING THE RESULTS

Although high gradient was not achieved in the accelerating mode during the test, valuable information was gathered that later helped us find the source of the problem. Unloaded quality factors for 4 of the 5 passband modes were calculated and can be compared with theoretical values. In order to

obtain the theoretical values for  $Q_0$ , the following expression for BCS resistance was used [1]:

$$R_{BCS} = 2 \times 10^{-4} \frac{1}{T} \left( \frac{f}{1.5} \right)^2 \exp\left(-\frac{17.67}{T}\right), \quad (1)$$

where  $f$  is the RF frequency in GHz, and  $T$  is temperature in K. At the altitude of Los Alamos, atmospheric pressure is about 80% of normal, which corresponds to a helium boiling temperature of 4.0 K. Total resistance  $R_s$  is given by the sum of  $R_{BCS}$  and  $R_0$  – residual resistance, which is assumed to be equal to a typical value of 10 n $\Omega$ . The unloaded  $Q$  is equal to  $G/R_s$ , where the geometry constant  $G$  can be calculated with HFSS. We computed theoretical  $Q$ -factors for the passband modes and compared them to the measured values (Table 2).

Table 2: Unloaded  $Q$  Factors

Passband mode	Theoretical $Q_0$	Measured $Q_0$
$\pi/5$	$2.0 \times 10^8$	not measured
$2\pi/5$	$2.4 \times 10^8$	$2.2 \times 10^8$
$3\pi/5$	$2.1 \times 10^8$	$9.3 \times 10^5$
$4\pi/5$	$2.3 \times 10^8$	$2.7 \times 10^8$
$\pi$	$2.2 \times 10^8$	$1.6 \times 10^6$

The measured  $Q$ -factors for the modes  $2\pi/5$  and  $4\pi/5$  agree reasonably well with theoretical predictions, while the measured  $Q$ -factors for modes  $3\pi/5$  and  $\pi$  are about 2 orders of magnitude lower than the prediction. This indicates that  $Q_{0,3\pi/5}$  and  $Q_{0,\pi}$  are limited by some non-superconducting losses.

## IMPROVED RF JOINT DESIGN

In order to understand where the source of the losses was, we looked at gradient profiles for the 4 modes (Fig. 7). It can be seen on the plot that the 2 modes that are not affected by the losses, have small field in the PBG cell, while the two modes with a low  $Q_0$  have a field in the PBG cell comparable in magnitude to fields in the other cells. This is a strong indication that the source of the losses is located in the PBG cell.

SRF PBG single cells were fabricated previously by Niowave, successfully tested and had high  $Q$ -factors [8,9]. This time we followed a very similar fabricating procedure. The only significant difference is the waveguide couplers added to the periphery of the PBG cell.

For the vertical test, all 3 waveguides were covered with niobium plates that, once squeezed, were supposed to provide an RF seal (Fig. 8). The  $4\pi/5$  and the  $\pi$  modes are confined inside the PBG array and have negligible fields at niobium plates that cover HOM waveguides. However, there is a significant field on the FPC cover due to the removed PBG rod (as can be seen on Fig. 1). This makes the FPC cover the most likely place to produce high losses.

It is necessary to mention that a conventional way to cover waveguide ports for a high gradient test involves using an

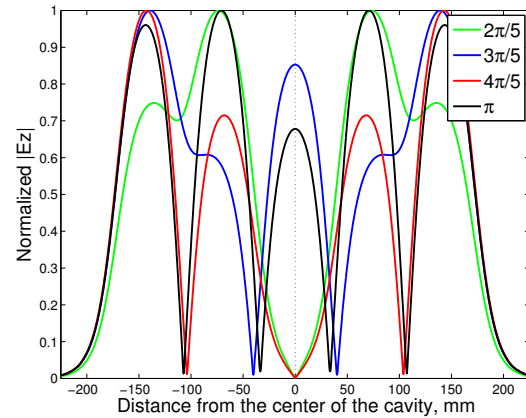


Figure 7: Simulated gradient profiles for the 4 measured passband modes.

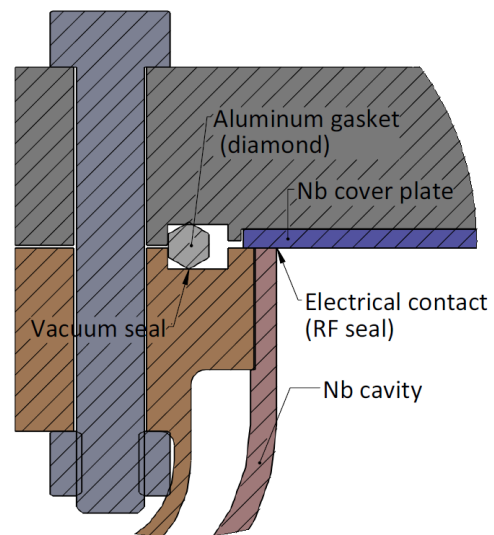


Figure 8: FPC waveguide cover, also seen encircled in Fig. 5. Niobium-to-niobium contact provides an RF seal, while a "diamond" gasket provides a vacuum seal.

indium gasket for both a vacuum and an RF seal (as in, for example, [13]). However, indium gaskets have the disadvantage of leaving residue on RF flanges. Therefore a different idea was implemented with vacuum and RF seals provided by different parts of the joint; clamped niobium-to-niobium contact provides an RF seal, as in [14], and a «diamond» aluminum gasket provides a vacuum seal, as in [15].

We define the quality factor associated with just the losses in the joint  $Q_{joint} = \omega U / P_{joint}$ , where  $\omega$  is the angular frequency,  $U$  is the total energy stored in the cavity and  $P_{joint}$  is the power lost in the joint. We can then separate the two contributions to the unloaded  $Q$  factor:

$$\frac{1}{Q_0} = \frac{1}{Q_{cav}} + \frac{1}{Q_{joint}}, \quad (2)$$

where  $Q_{cav}$  is related to the "normal" losses in the cavity walls.

In the superconducting experiment  $Q_0$  for the accelerating mode was dominated by the joint losses due to the fact that  $Q_{joint} \ll Q_{cav}$ . However, the opposite is true for a room temperature test. This makes diagnosing the problem more complicated as at room temperature changes in the joint design would not cause any noticeable changes in  $Q_0$ . In order to avoid doing multiple superconducting experiments to diagnose the problem, an indirect approach involving a trapped waveguide mode was used.

The trapped waveguide mode at 1.777 GHz is localized close to the joint (Fig. 9). Therefore, while having a field pattern at the joint similar to the  $\pi$  mode, its  $Q_0$  is much more sensitive to changes in joint losses. The mode can be excited with long and bent antennas that go through the beam pipes of the cavity. The Q factor can then be calculated from the width of the  $S_{21}$  curve.

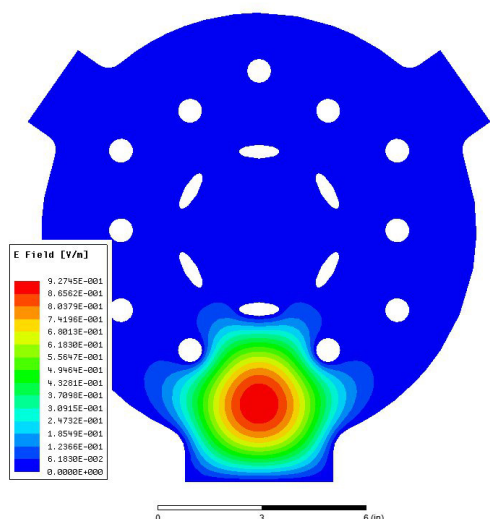


Figure 9: Magnitude of the E field of the trapped waveguide mode, shown on a plane that goes through the center of the PBG cell. The mode is an effective tool in diagnosing the low Q problem.

The measured Q factors for the trapped mode are summarized in Table 3. For the case of zero joint losses,  $Q_0$  (equal to  $Q_{walls}$ ) can be estimated using niobium conductivity at room temperature  $6.57 \times 10^6 \Omega^{-1}$  and the geometry constant  $G = 187 \Omega$  of the mode. The measured value, however, was much smaller than that estimate and varied greatly when the niobium cover plate (shown in blue on Fig. 8) was manually pressed down to the cavity.

Table 3: Quality factors for the trapped waveguide mode.

	$Q_0$
Expected value for the case of zero joint losses	5710
Measured value for the old (poor) joint	140
Measured value for the new joint	5650

Tests with various joint configurations showed that such an unusually low Q is not related to the mode radiating away or Ohmic losses in the walls. Rather, the losses are related to poor electrical contact between the walls of the cavity and the covering niobium plate. The poor contact was a result of the cover plate only touching the cavity walls at a few points, as opposed to a uniform contact along the entire perimeter. The actual nature of the losses may be related to an oxidation layer of  $Nb_2O_5$  that forms on the surface of niobium.

Once the problem was identified, a number of different solutions were suggested. The solution that was implemented consists of several steps. First, the shape of the niobium plate was modified to improve the RF contact as the plate is pressed to the cavity. Second, an adjustment was made to the depth of the groove for the aluminum gasket. Finally, tolerances were improved to ensure that both aluminum and niobium gaskets are crushed the same amount. The new design was shown to work at room-temperature tests. Table 3 shows the final Q of the trapped mode.

## CONCLUSIONS

This paper reported the first SRF multi-cell accelerating cavity with a PBG coupling cell has been designed with an emphasis on HOM damping and high real estate gradient. The niobium cavity was fabricated and tuned to the desired gradient profile. The cavity has been tested at cryogenic temperatures, but the test was unsuccessful. The accelerating mode showed an abnormally low Q-factor, inconsistent with the predicted BCS losses. Joint losses at the cavity-waveguide interface for fundamental power coupling can explain the test results, and an improved RF seal has been implemented. Another vertical test is scheduled in October 2015 to obtain the missing data on unloaded Q factors and accelerating fields.

## REFERENCES

- [1] Hasan Padamsee, Jens Knobloch and Tom Hays, "RF Superconductivity for Accelerators", Second Edition, Wiley-VCH (2011).
- [2] Sergey Belomestnykh et al, "On the frequency choice for the eRHIC SRF linac", Proceedings of IPAC 2014.
- [3] Thomas P.Wangler, "RF Linear Accelerators", Second Edition, Wiley-VCH.
- [4] Evgenya I. Smirnova, "Novel Photonic Band Gap Structures for Accelerator Applications", PhD Thesis, Massachusetts Institute of Technology, June 2005.
- [5] JieXi Zhang et al, "Design and High-Power Testing of a Hybrid Phoronic Band-Gap Accelerator Structure at 17 GHz", WEPWA062, Proceedings of IPAC 2015.
- [6] Carl A.Bauer et al, "Truncated Photonic Crystal Cavities with Optimized Mode Confinement", J. Appl. Phys. 104, 053107 (2008).
- [7] Evgenya Simakov et al, "Experimental Study of Wakefields in an X-Band Photonic Band Gap Accelerating Structure", WEPJE008, Proceedings of IPAC 2015.

- [8] Evgenya Simakov et al, "First High Power Test Results for 2.1 GHz Superconducting Photonic Band Gap Accelerator Cavities", Phys. Rev. Lett. 109, 164801 (2012).
- [9] Evgenya Simakov et al, "Raising gradient limitations in 2.1 GHz superconducting photonic band gap accelerator cavities", Appl. Phys. Lett. 104, 242603 (2014).
- [10] Haipeng Wang et al, "Simulations and Measurements of a Heavily-damped Multi-cell SRF Cavity", WEPMS070, Proceedings of PAC 2007.
- [11] Sergey A. Arsenyev, Evgenya I. Simakov, "Update on the design of a five-cell superconducting RF module with a PBG coupler cell", WEPAC34, Proceedings of NAPAC 2013.
- [12] Sergey A. Arsenyev et al, "Five-cell Superconducting RF Module with a PBG Coupler Cell: Design and Cold Testing of the Copper Prototype", Proceedings of IPAC 2015.
- [13] Haipeng Wang et al, "CRAB cavity and cryomodule prototype development for the advanced photon source", WEOCS7, Proceedings of PAC 2011.
- [14] W.Hartung et al, "Niobium Quarter-Wave Resonator Development for the Rare Isotope Accelerator", TUP14, Proceedings of SRF 2003.
- [15] L.Monaco et al, "Experimental and theoretical analysis of the TESLA-like SRF cavity flanges", MOPCH170, Proceedings of EPAC 2006.